Co-occurrence of marine heatwaves and cold-spells between nearshore and offshore regions of South Africa

Robert W. Schlegel[a,*], Eric C. J. Oliver[b,c], Thomas W. Wernberg[d], Albertus J. Smit[a]

[a]*Department of Biodiversity and Conservation Biology, University of the Western Cape, Private Bag X17, Bellville 7535, South Africa*
[b]*ARC Centre of Excellence for Climate System Science, Australia*
[c]*Institute for Marine and Antarctic Studies, University of Tasmania, Hobart, Australia*
[d]*UWA Oceans Institute and School of Plant Biology, The University of Western Australia, Crawley, 6009 Western Australia, Australia*

Abstract

As climates change it is necessary that we understand the new threats that this may create. The shallow water ecosystems found along the coastlines of the world are particularly at risk as their temperatures may change more rapidly and dramatical than waters in the open ocean. To this end it is necessary that we identify the occurrence of extreme events, referred to here as Marine Heatwaves (MHWs) and Marine Cold-Spells (MCSs), in the nearshore environment as both strong warm and cold events may be damaging to local flora and fauna. We have taken a recently developed algorithm that defines these extreme events in a novel way and applied it to the *in situ* time series available for the coast of South Africa that are longer than 10 years and with at least 90% complete daily records. We found that MHWs and MCSs occur along the entirety of the coast of South Africa and with some temporal and spatial agreement between the largest events detected. MHWs occur more often, last longer and have greater cumulative intensities than MCSs. The cumulative intensity [°C × days] for most MHWs and MCSs were comparable however, several were much larger and there tended to be specific areas that displayed more extreme events than the coastal average. The coast was further divided into three sections (west, south, and east) to investigate the effect of geography and differing oceanographic conditions on MHWs and MCSs and it was found that the south coast experiences longer, more intense and a greater count of MHWs and MCSs than the other two coastal sections. The mechanism driving the higher intensity of events on the south coast requires further study. The largest three MHWs in each of the time series along the coast of South Africa have generally occurred in the second half of the time series whereas the largest three MCSs have generally occurred in the first half. Thus implying that MHWs are on the rise while MCSs are declining. These same calculations were conducted for offshore temperatures from NOAA Optimally Interpolated sea surface temperature (OISST) data at the nearest locations to the *in situ* stations and it was found that a similar pattern of increasing MHWs and decreasing MCSs existed. An additional finding was that the proportion of co-occurrence between *in situ* and OISST data for each coastal section ranged from 0.20–0.50 with co-occurrence rates for both MHWs and MCSs being the largest on the south coast. Most individual time series

*Corresponding author
Email address:* `3503570@myuwc.ac.za` (Robert W. Schlegel)

showed co-occurrence rates between 0.25–0.50 for both MHWs and MCSs with co-occurrence rates generally higher for MHWs.

---

1. Introduction

Over the past three decades, anthropogenically mediated warming has negatively affected marine and terrestrial realms with far reaching consequences for humanity and natural ecological functioning. Although climate change is generally understood as a gradual long-term rise in global mean surface temperature (Pachauri et al., 2014), which will continue for decades or centuries, it is generally the associated increase in the count and severity of extreme events that affects humans and ecosystems in the short-term (Easterling et al., 2000). Impacts of extreme events such as floods, wind storms, tropical cyclones, heatwaves and cold-spells are often sudden with catastrophic consequences. 'Pulse' events exceeding certain thresholds of count, intensity, duration, timing and rate of onset can drive punctuated perturbations to species distributions, which eventually modify the structure and function of ecosystems (Wernberg et al., 2013; Rehage et al., 2016), and the recognition to focus more on the extremes and less on the background mean state has emerged as a recent direction of climate change research (Jentsch et al., 2007).

'Heatwaves' usually refer to atmospheric phenomena where vague definitions such as "a period of abnormally and uncomfortably hot weather" are invoked (American Meteorological Society, 2011), but there are also precise definitions based on statistical properties and other metrics of the temperature record that are relative to location and time of year (e.g. Meehl, 2004; Alexander et al., 2006; Fischer and Schär, 2010; Fischer et al., 2011; Perkins and Alexander, 2013). Recent years have seen investigations of heatwaves in the ocean due to them becoming more frequent (e.g. Mackenzie and Schiedek, 2007; Selig et al., 2010; Sura, 2011; Lima and Wethey, 2012; DeCastro et al., 2014). Well-known marine heat waves (MHW) have occurred in the Mediterranean in 2003 (Black et al., 2004; Olita et al., 2007; Garrabou et al., 2009), off the coast of Western Australia in 2011 (Feng et al., 2013; Pearce and Feng, 2013; Wernberg et al., 2013), in the north west Atlantic Ocean in 2012 (Mills et al., 2012; Chen et al., 2014, 2015) and now the "Blob" from 2014 to 2016 in the north east Pacific Ocean (Bond et al., 2015). The extreme temperatures from these events may have negative impacts upon the local ecology for the regions in which they occur. For example, the 2003 Mediterranean heatwave may have affected up to 80% of the gorgonian fan colonies in certain areas of this sea (Garrabou et al., 2009), whereas the 2011 event off the west coast of Australia has been recognized as being a driving factor in the regime shift there from temperate kelp forests to the beginnings of a coral reef system (Wernberg et al., 2013). The extensive bleaching of corals in early 2016 has also been attributed to masses of anomalously warm waters (refs.).

Although the consequences of these anomalously warm events are widely publicised, the events themselves have until recently not been objectively characterised. Consequently, Hobday et al. (2016)

have defined MHWs as "a prolonged discrete anomalously warm water event that can be described by its duration, intensity, rate of evolution, and spatial extent", and in doing so have derived statistical metrics that characterise these properties. For example, the count of MHWs within a time series and their maximum and cumulative intensity are quantifiable parameters that can be calculated in a consistent manner irrespective of geographical location. Practically, we are now able to determine thresholds of certain metrics, which when exceeded, can be linked to impairments and alterations of ecological systems. The focus of this paper is on marine thermal events that are extreme with respect to the seasonal climatology as per the Hobday et al. (2016) definition. They may be anomalously warm events, or anomalously cold (marine cold-spells, MCSs; introduced here). While MHWs are becoming reasonably well known by virtue of their increasing frequency and intensity, MCSs have received less recognition. Whereas extreme hot events may be demonstrably damaging to organisms and ecosystems, extreme cold events also have the potential to negatively impact organisms and ecosystems. In both cases their drivers and dynamics, particularly in the coastal zone, remain poorly understood.

MCSs are projected to become less frequent under future climatic scenarios, but there are also examples of them becoming more frequent in some localities (e.g. Gershunov and Douville, 2008; Matthes et al., 2015). They are frequently lethal (Woodward, 1987) and are known to have caused mass fish (Gunter, 1941, 1951; Holt and Holt, 1983) and invertebrate (Gunter, 1951; Crisp, 1964) kills, the death of juvenile and sub-adult manatees (O'Shea et al., 1985; Marsh et al., 1986) as well as affecting organismal physiological tolerances, life history strategies, and habitat requirements (Ellis, 2015). Cold temperatures are very important in setting species population distribution limits, particularly limiting their range north- or southwards towards high latitudes (Firth et al., 2011), and the timing of the onset of the growing season (Jentsch et al., 2007). It is easy to postulate how population-level consequences might aggregate to drive whole ecosystem responses (e.g. Kreyling et al., 2008; Rehage et al., 2016). Indeed, the range contractions of ecosystem engineer species such as mussels have been shown to relate to MCSs (Firth et al., 2011, 2015).

Some of the MCSs known to have impacted populations were caused by cold-spells affecting the intertidal and coastal biota locally (Gunter, 1941; Firth et al., 2011). We hypothesise that these localised events are manifestations of extreme atmospheric warm or cold weather phenomena situated over the coast. On the other hand, we think that broader-scale drivers may also affect the thermal properties and dynamics of coastal systems. There is by no means a good understanding of the relative contributions of local- *vs.* broad-scale drivers of coastal MHWs and MCSs, as such studies have not yet been undertaken to the best of our knowledge. The origin of MHWs at any scale seems conceptually straight forward: it seems likely that they result directly from atmosphere-ocean heat transfer. In a world that is warming, their intensity and frequency will increase over time when their magnitude is computed relative to a long-term climatology. But what about MCSs — in a warming world, why would their intensity/frequency increase? The answer to this question probably lies with physical ocean processes that influence the redistribution of heat. For example, large-scale atmospheric-oceanographic coupling is being affected by global warming, which is projected to cause the intensification of upwelling

favourable winds and consequently the intensification and increasing count of upwelling events (see García-Reyes et al., 2015, for a review of this and alternative hypotheses). We therefore propose that the development of coastal MCSs can be attributed to an intensification of upwelling. Since MHWs and MCSs are both able to effect ecosystem change, a mechanistic understanding of their drivers will be invaluable. To this end our study serves as a constructive first step to understand the prevalence of anomalous thermal events with respect to forcing mechanisms at different scales.

Hobday et al. (2016) applied their MHW framework to ¼° NOAA optimally interpolated sea surface temperature data (hereafter referred to as OISST; Reynolds et al., 2007), but warned users to be cognisant that different data sets would provide different kinds of information pertaining to heatwaves. Our study applies the MHW (MCS) definition to datasets of coastal *in situ* (local-scale) and offshore gridded SST (broad-scale) temperature time series collected at different locations along coastlines influenced by contrasting ocean currents — the Benguela Current, an eastern boundary upwelling system, and the Agulhas Current — and locally modified by regional aspects of the coastal bathymetry and geomorphology and other smaller scale coastal features. These systems, assessed within a framework that couple local- and broad-scale features, permit us to assess how MHWs (MCSs) develop in coastal regions. Specifically, we aim to assess the significance of MHWs (MCSs) within the context of i) the data sets' inherent differences, ii) the various dynamical properties that then emerge out of the regional oceanographic context, and iii) out of the local-scale modifications of the regional ocean features as they approach the coast. In doing so, we wish to provide a mechanistic understanding of the nature and origin of MHWs (MCSs) within oceanographically distinct ocean/coastal regions. The working hypothesis is that MHW and MCS manifesting offshore and onshore are decoupled (no difference in timing, duration, frequency and intensity). We predict that coastal MHW events are coupled with synoptic scale ocean thermal patterns visible across the offshore region at scales of 100s of kilometres, and that MCS originate at a local scale as isolated incidents. The possibility of atmospheric forcing on coastal events is considered a very likely possibility but it was not assessed within the scope of this study.

2. Methods

2.1. Study region

The variety of oceanographic features around the *ca.* 2,700 km long South African coast provides a natural testing bed for the potential effects of different ocean forcing mechanisms on the occurrence of MHWs and MCSs. Annual mean (standard deviation; hereafter referred to as "sd)" coastal seawater temperatures range from 12.3 (1.2)°C at the western limit near the Namibian border (Site 1) to 24.4 (2.0)°C in the east near the Mozambican border (Site 21), and our study sites were selected to cover this full range (Figure 1). We classify the coast into three regions based on their major oceanographic features, their temperature characteristics, and aspects of the underlying continental shelf. The first is the west coast region dominated by the Benguela Current, which forms an Eastern Boundary Upwelling System (EBUS) (Hutchings et al., 2009). Seasonal upwelling is maintained by prevailing

south-easterly trade winds. Evenly low temperatures are especially noticeable at upwelling cells over a

relatively narrow continental shelf in the region northwards of the Cape Peninsula to Cape Columbine. The west coast defines a cool temperate regime, with the range of monthly mean temperatures at most sections intermediate between cold temperate and warm temperate (Lüning, 1990). The second region is the warm temperate (Lüning, 1990) east coast where the influence of the south-westerly flowing warm Agulhas Current flowing tightly along the narrow continental shelf (except for the Natal Bight) is strongly felt. This stretch of coast is spatially homogeneous with respect to temperature and characterised by a moderate amount of seasonal variation. Although the Agulhas Current retroflects back into the southern Indian Ocean (Hutchings et al., 2009) just south of the much wider and cooler Agulhas Bank (Roberts, 2005), its influence regularly extends as far west as False Bay (Sites 5–21; Figure 1). The third coastal region is that overlying the Agulhas Bank. Although also warm temperate, it experiences a much larger range in annual temperature and variability compared the west and east coast regions, which is in part influenced by the retention and cooling of Agulhas Current water on the bank, the presence of some current-driven upwelling cells along this coastal section (Sites 15–17) (Roberts, 2005), and because of the effects of embayments and capes throughout the region.

2.2. Temperature data

We use two sources of seawater temperature data. The first dataset is comprised of 127 records of *in situ* temperature records of daily measurements for up to 40 years in duration with a mean duration of *ca.* 19 years. Whereas these *in situ* time series are generally shorter than the recommended 30 year minimum (Hobday et al., 2016) and have some small amounts of missing data, it is our opinion that the benefit of using *in situ* data over satellite data is that they give a better representation of the temperatures felt by coastal ecosystems as well as the thermal characteristics near the coast, a region where satellite SST measurements have been shown to perform poorly (e.g. Smale and Wernberg, 2009; Castillo and Lima, 2010). In a South African context, Smit et al. (2013) have shown that satellite SST data display a warm bias as large as 6°C over *in situ* temperatures in the nearshore environment. In an attempt to compromise between the proscribed requirements in Hobday et al. (2016) of a 30 year minimum and making use of this valuable dataset, all time series under 10 years in duration were eliminated. We found 10 years to be the minimum duration required in order to generate a robust estimate of the climatology required for the identification of MHWs and MCSs. Next, the remaining time series were further screened and those missing more than 10% of their daily values were removed, leaving a total of 21 time series. Care was taken to select continuous series with as few as possible consecutive missing values, since having regions in the data with more than two consecutive missing data points interferes with the identification of the anomalous events (see below). These stations were classified into three coastal sections defined by properties of their oceanography and biogeography Smit et al. (2013). Details on the selected time series, including location, duration, and the coastal sections they were aggregated into may be found in Table S1 and the site localities are displayed spatially in Figure 1.

Figure 1: Map of southern Africa showing the bathymetry (only the 250m isobath is labelled), the location of the *in situ* thermal time series shown with circles and approximations of the pixels used along the shore-normal transects from the daily ¼° NOAA OISST Reynolds et al. (2007) shown with black boxes. The JPL G1SST 1 km blended SST field shows the state of the ocean on 2016-02-14; this image was selected as it clearly shows the full range of ocean processes around southern Africa. The Agulhas Current along the east coast of the country is visualized here in a yellowish colour as a jet of relatively warmer water projecting in a south-westerly direction, and hugging the continental shelf. The blueish patches north of the Cape Peninsula represent upwelled water. Some upwelled water may also be present around Sites 14 (Tsitsikamma) and 15–16 (Port Elizabeth). The inset maps show detail of the Cape Peninsula/False Bay area and the Hamburg region where site labels are obscured due to overplotting of symbols.

The second set of temperature data used in this study are the daily ¼° NOAA optimally interpolated sea surface temperature (OISST; Reynolds et al., 2007) derived from the Advanced Very High Resolution Radiometer (AVHRR). To compare the offshore meso-scale (OISST dataset) extreme events against those along the coast (*in situ* dataset), shore-normal transects were drawn from each of the 21 sites extending to the 200m isobath. Temperature values from the OISST data were then extracted at each of the roughly 25×25 km pixels along these transects, shown as black boxes in Figure 1. Where the shelf was less than 25 km wide (Sites 17–21) the nearest 'ocean pixel' to the *in situ* time series coordinate was used. It was decided to use mean temperatures along these shore-normal transects as they better represent the meso-scale temperatures we were interested in comparing against the coastal events, rather than simply using the nearest OISST pixel, as this would only draw a comparison between the two different data types at the coast, and not the meso-scale activity in the ocean. The individual time series within each pixel of each transects were then averaged to create 21 time series to match against those calculated for the *in situ* sites. These 21 OISST time series could then be analysed for MHWs (MCSs) in the same way as the *in situ* data (see below). Note that the OISST time series had valid data covering 1982–2015 which did not match exactly the coverage by individual *in situ* sites.

2.3. Defining and calculating MHWs and MCSs

MHWs are defined here following Hobday et al. (2016) as "discrete prolonged anomalously warm water events in a particular location." MCS are defined in the same manner as MHWs with the exception of being "anomalously cold water events".

First, a climatological mean and 90th and 10th percentiles were calculated for each day of the year by pooling all data within an 11-day window across all years. MHWs (MCSs) were detected as periods of time when temperatures exceeded the 90th (10th) percentile for at least five days. The implication was therefore that MHWs (MCSs) could develop outside of the warm (cold) season (i.e. winter (summer) months). Since our *in situ* time series were of differing durations we calculated the climatology over all available years; in the case of the OISST data, climatologies were calculated over a fixed 33-year base period (1982–2015). Furthermore, discrete events with well-defined start and end dates but with 'breaks' between events lasting ≤2 days followed by subsequent ≥5 day events were considered as continuous events. After the events were defined, a set of metrics (Table 1) were calculated including maximum and mean intensity (measured as anomalies relative to the climatological mean, in °C), duration (days from start to end dates, in days), and cumulative intensity (the integrated intensity over the duration of the event analogous to degree-heating-days, in °C). Although MCS intensities are calculated as negative values (i.e. anomalies) they are reported here as absolute values.

A Python script (https://github.com/ecjoliver/marineHeatWaves; see Hobday et al., 2016) was used to calculate the individual MHWs for both the *in situ* and OISST time series. The script was modified to permit the calculation of MCSs. After the individual events were recorded, mean annual values for the metrics seen in Table 1 were created for each year of each times series. This provided two different sets of measurements for the extreme events that will be referred to specifically throughout this paper. 'Annual' data refers to the annual means of events for each year of each time series whereas

7

Table 1: Metrics of MHWs and their descriptions as used by Hobday et al. (2016). In the case of MCSs, values are calculated with respect to the 10th percentile and absolute intensity values are reported.

Name [unit]	Definition
Count [no. events per year]	n: number of MHWs per year
Duration [days]	D: Consecutive period of time that temperature exceeds the threshold
Maximum intensity [°C]	i_{max}: highest temperature anomaly value during the MHW
Mean intensity [°C]	i_{mean}: mean temperature anomaly during the MHW
Cumulative intensity [°C]	i_{cum}: sum of daily intensity anomalies over the duration of the event

'event' data refer to the individually calculated events that have not been aggregated into annual
means.

Because MHWs (MCSs) are calculated by percentiles, rather than absolute definitions such as periods with temperatures above an arbitrary fixed temperature threshold, any time of year could be shown to be experiencing a MHW (MCS). This is an important consideration as unusually warm waters occurring during the winter months of a year, the time when many species need cold water for effective spawning/spore release, can have a negative effect on the recruitment success of that population for the year (Wernberg et al., 2011).

2.4. Detecting co-occurrence of coastal and offshore events

In order to better understand the potential impact mesoscale phenomena have on coastal events, the proportion of co-occurrence between the MHWs (MCSs) found within each time series between the two datasets was calculated. This was initially done by taking each event (warm and cold) within an *in situ* time series and looking for an event occurring within the OISST time series at the same site within a certain period of time before the *in situ* date. These co-occurrence proportions were used to describe how often the mesoscale oceanography off the coast led the extreme events occurring along the coast. All events occurring on dates outside of the dates occurring within the matching time series were removed from this calculation. The sum of events found to occur within the same time frame was then divided by the total number of *in situ* events that occurred during the time period shared with the OISST data (which varies from station to station) to produce a co-occurrence proportion. The proportions of co-occurrence were then recalculated controlling for the size of the lag window used when comparing the two different datasets for concurrent events, as well as the directionality used for this comparison. In other words, a range of window sizes from 2-14 were used for each site to see how far apart events generally occurred and the lag period used was also applied only after the *in situ* date, as well as both before and after the date, effectively doubling the range of the lag. This allowed us to see how often the *in situ* event led the mesoscale event as well as seeing broadly the amounts of co-occurrence occurring between the two data sets.

Besides controlling for the duration and direction of lag, the size of the events themselves (ranked by cumulative intensity) was compared. This was accomplished by controlling the pool of events with which to compare the datasets per site in steps of 10th percentiles. This progressively removed smaller events until only the larger events were being compared. This allowed us to track the co-occurrence of only the largest events, reducing the overall proportion of co-occurrence found within each site as

Table 2: The mean(sd) values for event count, duration and mean intensity from the annual data for MHWs and MCSs for each coastal section as calculated from the *in situ* time series. The aforementioned annual data were averaged across all years for all time series within each respective coast to produce the mean (sd) values shown in this table.

coast	MHW [count]	duration [days]	mean intensity [°C]	MCS [count]	duration [days]	mean intensity [°C]
all	1.6(1.8)	9.3(5.1)	2.65(0.79)	1.5(1.7)	9.0(5.1)	2.79(1.09)
west	1.8(1.9)	9.1(3.9)	2.86(0.90)	1.5(1.9)	8.5(5.2)	2.32(0.58)
south	1.5(1.8)	9.8(6.1)	2.50(0.65)	1.5(1.6)	9.7(5.5)	3.08(1.22)
east	1.5(1.7)	7.7(2.2)	2.85(0.89)	1.6(1.6)	7.1(1.9)	2.37(0.67)

caused by the smaller events occurring at similar times as large events.

The top three MHWs (MCSs) for each *in situ* and OISST time series as defined by cumulative intensity were also noted in order to visually compare the co-occurrence of events in detail, both within and between the different datasets.

Given that the anthropogenic forcing of climate change is predicted to increase the temperature of most of the ocean over time, it stands to reason that, as a function of the 90th and 10th percentiles, one would expect to see the larger MHWs near the end of the time series, and the larger MCSs near the beginning. This can be tracked visually by looking at the top three warm and cold events for each time series. Given that the OISST time series are greater than 30 years in duration it is possible to discern the long term trends within the data apart from the noise of any inter-decadal patterns (Schlegel and Smit, in review). Using a simple linear model, the decadal trend in the annual occurrence of MHWs and MCSs was calculated for all of the OISST data as well as the *in situ* time series that were over 30 years long. The shorter time series simply had the proportion of MHWs or MCSs in the first half of the time series compared against those in the second half to show if there were more or fewer.

3. Results

3.1. Events

Table 2 shows that the *in situ* time series representing the typically cooler west coast experienced longer and more intense MHWs, on average, than those along the other two coastal sections. On the other hand, the volatile south coast experienced the longest and most intense MCSs. There was no significant difference between the annual count of events for each coastal section (F=0.727, df_1=2, df_2=926, p=0.48) or between the count of MHWs and MCSs (F=0.732, df_1=1, df_2=926, p=0.39). There was a significant difference between the coastal sections for the duration of events (F=8.907, df_1=2, df_2=594, p<0.01) but the difference in duration of MHWs and MCSs was not significant (F=0.722, df_1=1, df_2=594, p=0.39). The intensity of events was significantly different between each coastal section (F=57.55, df_1=2, df_2=594, p<0.01) and the type of events (F=5372, df_1=1, df_2=594, p<0.01). Note that the degrees of freedom in the results for the count of events and duration/intensity differ as there were long stretches of time series in which there were no events. These were reported as 0 for the count results; however, any years in which no events occurred had their resultant duration and intensity of events reported as NA.

9

Table 3: The mean(sd) values for event count, duration and mean intensity from the annual data for MHWs and MCSs for each coastal section as calculated from the OISST time series. The aforementioned annual data were meaned across all years for all time series within each respective coast to produce the mean(sd) values shown in this table.

coast	MHW [count]	duration [days]	mean intensity [°C]	MCS [count]	duration [days]	mean intensity [°C]
all	2.2(2.1)	10.2(5.4)	1.72(0.33)	2.2(2.6)	10.2(5.1)	1.83(0.52)
west	2.1(1.8)	10.9(6.7)	1.75(0.41)	2.3(2.7)	9.8(6.6)	1.87(0.61)
south	2.2(2.1)	10.6(5.5)	1.74(0.29)	2.1(2.7)	10.7(5.0)	1.79(0.45)
east	2.5(2.3)	8.3(2.4)	1.64(0.33)	2.2(2.2)	9.4(3.4)	1.93(0.61)

[Contradictions...] Results from the analysis of the OISST data (Table 3) show that there was a significant difference from the *in situ* data for count (F=50.27, df_1=1, df_2=2306, p<0.01) and duration (F=17.57, df_1=1, df_2=1612, p<0.01) of events but not mean intensity (F=0.117, df_1=1, df_2=1612, p=0.73). The mean annual count and duration of MHWs and MCSs were greater than their *in situ* counterparts for all coastal sections whereas the intensity of both event types on all coastal sections were less than that of the *in situ* data. With this in mind we still see that the pattern of MHW and MCS event sizes along the coast differed from the *in situ* data, too. The largest annual number of MHWs in the OISST data occurred on the warmer east coast whereas the longest MHWs occurred on the volatile south coast with the most intense events nearly split between the west and south coasts respectively. The cooler west coast saw the most frequent occurrence of MCSs with the OISST data. The longest MCSs occurred on the south coast, same as the *in situ* data however, the most intense MCSs were seen off the east coast. There was no significant difference between the annual count of events per coast (F=0.542, df_1=2, df_2=1380, p=0.58) or event type (F=0.155, df_1=1, df_2=1380, p=0.69). The duration of the events in the different coastal sections differed significantly from one another (F=9.534, df_1=2, df_2=1018, p<0.01) whereas the duration of the event types did not (F=0.055, df_1=1, df_2=1018, p=0.81). Lastly, as with the *in situ* data, the intensity of the events from the OISST dataset differed significantly between each coastal section (F=16.17, df_1=2, df_2=1018, p<0.01) and the type of event (F=17645, df_1=1, df_2=1018, p<0.01).

3.2. Top three events

The mean annual statistics shown in Table 2 and Table 3 give a broad overview of the events occurring along the coast; however, examining the largest MHWs and MCSs better aids in our understanding of which coastal sections show the most intense events. The ranking of these events is based on the cumulative intensity (°C) metric as explained in Table 1. The three largest MHWs that occurred within the *in situ* dataset were all on the south coast (Table 4). Two of these events occurred during 1999, making it a particularly hot year. The size of the south coast events are larger than those occurring along the west coast, with the largest three MHWs on the east coast being much smaller than those occurring on the south coast (Table 4). This is unsurprising as one may see in Table 4 that the duration of events on the south coast are longer that those on the west and east coasts. The cumulative intensity of the entire coast and each section individually may be calculated for both datasets from Table 2 and Table 3 by multiplying the duration by the intensity. When calculating

Table 4: The three largest MHWs per coast from the *in situ* data. The coast column shows in which coastal section the event occurred. The site column gives the name of the site, as seen in Figure 2, which gives the index number necessary to find it's location along the coast in Figure 1. The start date column gives the day on which the event began and the duration (days) column shows how many days the event lasted for. The mean intensity and cumulative intensity columns are explained in Table 1.

coast	site	start date	duration [days]	mean intensity [°C]	cumulative intensity [°C x days]
west	Sea Point	1996-01-04	40	3.08	123.20
west	Sea Point	2005-05-21	39	2.56	99.66
west	Sea Point	1975-12-30	38	2.62	99.41
south	Muizenberg	1999-12-01	98	3.17	310.30
south	Mossel Bay	1993-06-25	97	1.77	171.30
south	Muizenberg	1999-10-20	35	4.47	156.40
east	Nahoon Beach	1995-10-14	18	5.18	93.31
east	Eastern Beach	1985-12-27	19	3.33	63.18
east	Orient Beach	1990-06-25	12	3.80	45.59

Table 5: The three largest MCSs per coast from the *in situ* data. Column descriptions may be found in the caption for Table 4.

coast	site	start date	duration [days]	mean intensity [°C]	cumulative intensity [°C x days]
west	Sea Point	1990-06-23	44	2.88	126.60
west	Sea Point	1983-06-10	39	2.84	110.90
west	Sea Point	2000-11-28	23	3.70	85.04
south	Muizenberg	1984-07-14	63	2.92	183.70
south	Muizenberg	1992-03-24	56	2.78	155.60
south	Ystervarkpunt	2000-05-11	51	2.94	150.10
east	Sodwana	2004-02-12	17	3.25	55.20
east	Orient Beach	1984-03-31	13	3.73	48.44
east	Orient Beach	1995-12-6	15	3.01	45.13

the mean cumulative intensity of MHWs from the *in situ* data for the entire coast by the individual events and not the annual means we see that mean(sd) is 26.11(24.37)(°C x days).

As with the MHWs, the largest three MCSs from the *in situ* data were also found on the south coast (Table 5). Maintaining the pattern seen with the MHWs, the largest MCSs on the west coast were the next largest three events for the entire coast with the three largest MCSs from the east coast being smaller than the other two coastal sections (Table 5). The pattern of the largest south coast events having a greater duration than the other coasts persists with the MCSs but is less pronounced. The mean(sd) cumulative intensity (°C x days) for MCSs over the entire coastal was 26.45(24.25)(°C x days). The cumulative intensity (°C x days) of events from each of the coastal sections in the *in situ* data were found to be significantly different (F=7.377, df_1=2, df_2=1444, p<0.01) as well as the events themselves (F=1753, df_1=1, df_2=1444, p<0.01).

As can be seen in Figure 2, the three largest events occurring for each time series within the OISST dataset are often different from the *in situ* dataset and show a greater amount of co-occurrence for neighbouring coastal stations than the corresponding *in situ* time series. This apparent difference in the cumulative intensity (°C x days) of events between the two datasets is significant (F=8.857, df_1=1, df_2=4493, p<0.01). The pattern seen in the *in situ* data of the largest MHWs and MCSs occurring on the south, west and east coasts respectively is not repeated with the OISST dataset. Whereas the largest MHW occurred on the south coast in the OISST data, the three largest MHWs from the west coast were larger than the second and third largest events from the south coast (Table 6). The
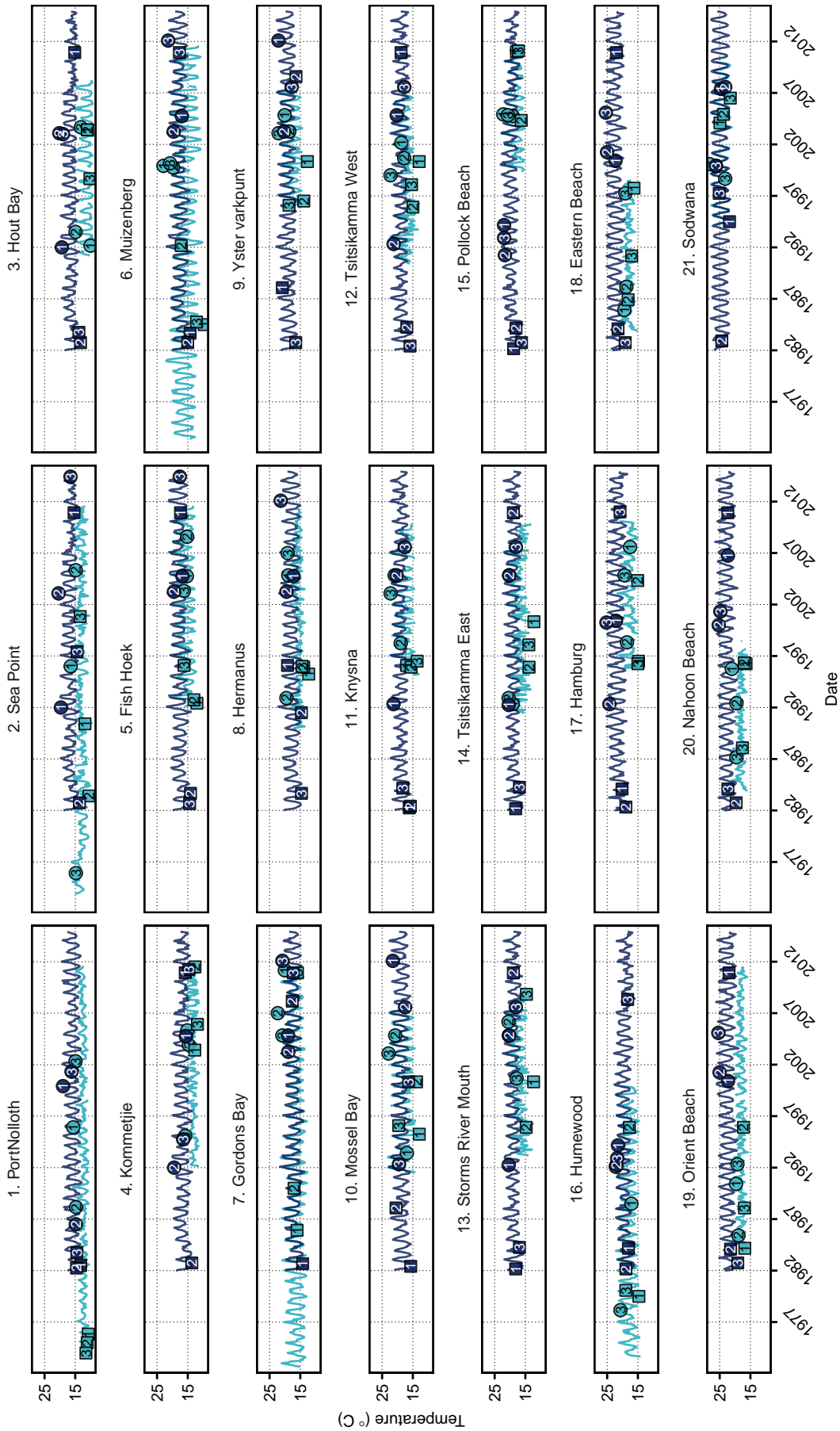
Figure 2: The daily temperature values for each *in situ* time series (light blue) used in this study and the corresponding OISST time series (dark blue) extracted for comparison as seen in Figure 1. The top three MHWs are indicated by circles (with the rank inside) for each site as judged by greatest cumulative intensity. The top three MCSs for each site are indicated by squares (with the rank inside). Sites 1 − 4 represent the west coast, sites 5 − 17 represent the south coast and sites 18 − 21 represent the east coast.

Table 6: The three largest MHWs per coast from the OISST data. Column descriptions may be found in the caption for Table 4.

coast	site	start date	duration [days]	mean intensity [°C]	cumulative intensity [°C x days]
west	Sea Point	1992-01-21	39	2.96	115.60
west	Hout Bay	1992-01-20	36	3.15	113.50
west	Kommetjie	2004-10-29	53	2.03	107.40
south	Knysna	1992-05-3	50	2.41	120.40
south	Fish Hoek	2004-10-30	53	1.92	101.60
south	Pollock Beach	1994-03-27	31	3.19	99.05
east	Nahoon Beach	2006-10-21	25	1.81	45.34
east	Eastern Beach	2000-06-24	26	1.58	41.12
east	Orient Beach	2000-06-24	26	1.58	41.12

Table 7: The three largest MCSs per coast from the OISST data. Column descriptions may be found in the caption for Table 4.

coast	site	start date	duration [days]	mean intensity [°C]	cumulative intensity [°C x days]
west	Kommetjie	2010-12-13	54	3.92	211.90
west	Hout Bay	2010-12-25	41	4.06	166.30
west	Sea Point	2010-12-25	41	3.78	154.90
south	Hamburg	1984-02-5	65	3.91	254.20
south	Storms River Mouth	1982-03-13	60	2.79	167.30
south	Tsitsikamma East	1982-03-13	60	2.79	167.30
east	Eastern Beach	2010-12-26	32	2.90	92.85
east	Orient Beach	2010-12-26	32	2.90	92.85
east	Eastern Beach	1984-02-24	22	3.97	87.26

three largest MHWs from the east coast again came in below the other coasts(Table 6). The mean(sd) cumulative intensity (°C x days) over the entire coastal for the MHWs from the OISST dataset was markedly lower than its *in situ* counterpart at 18.65(15.10)(°C x days).

The largest MCSs from the OISST data (Table 7) do not belong to the same coastal sections as their *in situ* counterparts (Table 5). The three largest MCSs on the east coast, with both datasets and both types of events, were smaller than the other two coasts (Table 7). All of the coastal sections show that at least two of their largest MCSs occurred at the same time at different sites. The coastal mean(sd) cumulative intensity (°C x days) of the MCSs from the OISST data were much closer to their *in situ* counterparts at 23.17(23.49)(°C x days). The difference in the cumulative intensity (°C x days) of events between the coastal sections in the OISST dataset were not found to be significant (F=0.503, df_1=2, df_2=3049, p=0.60) however, the difference between the MHWs and MCSs was (F=3472, df_1=1, df_2=3049, p<0.01).

The temperature values from the dates of the largest MHW and MCS for the west and south coasts from the *in situ* data may be seen concurrently with the temperature values from the matching OISST time series in Figure 3. One may see that when the largest events were occurring in the *in situ* data, the temperature values in the OISST data did not show similarly intense events.

3.3. Co-occurrence rates

The proportion of co-occurrence found for MHWs and MCSs between the datasets for each site may be seen in Figure 4 and Figure 5 respectively. When using the lag windows before and after the *in situ* event and comparing all events we see that as the width of the lag window increased from 2 to 14 days the mean proportion of co-occurrence for all sites increased linearly for MHWs (0.09 to 0.38 and

Figure 3: The temperature values from the *in situ* and OISST data during the largest MHW and MCS from the south and west coasts respectively from the *in situ* data. The left column shows the *in situ* temperature values during the event while the right column shows the OISST temperature values occurring on the same dates. The top row shows the largest MHW that occurred on the south coast while the second row shows the largest MHW that occurred on the west coast. The bottom two rows show the largest *in situ* MCS that occurred on the south and west coasts respectively.

MCSs (0.10 to 0.30). Using these same constraints we see that south coast sites had the largest mean increase in co-occurrence for MHWs (0.10 to 0.45) and MCSs (0.11 to 0.34) whereas the west coast sites showed the smallest increase for MHWs (0.07to 0.28) and MCSs (0.08 to 0.19). With all variables controlled for in the same manner, the co-occurrence rates between the different coastal sections were not significantly different for MHWs at a 2 day lag (F=0.799, df_1=2, df_2=18, p=0.46) or a 14 day lag (F=2.374, df_1=2, df_2=18, p=0.12). There were no significant differences between the coastal sections for MCSs at a 2 day lag (F=0.671, df_1=2, df_2=18, p=0.52) or 14 day lag (F=2.357, df_1=2, df_2=18, p=0.12).

The directionality of the lag window also affected the co-occurrence of events. Comparing all events within a 14 day lag window before the *in situ* event gave higher mean(sd) rates of co-occurrence for MHWs (0.22(0.13)) than for the same lag window after the *in situ* event for MHWs (0.18(0.10). This same comparison for MCSs showed that the lag window before the *in situ* event (0.16(0.09)) had slightly lower rates of co-occurrence than the lag window after the *in situ* event (0.17(0.08). When the smaller events were screened from comparison and only the largest half of the events were used (50th percentile), the difference in mean(sd) co-occurrence proportions for MHWs event lessened at 0.16(011) before the *in situ* event and 0.15(0.12) after. The mean(sd) co-occurrence proportion of MCSs at this level was less when using a lag window before the *in situ* event at 0.05(0.08) than for a lag window after at 0.08(0.08).

There was no co-occurrence for the largest MCSs between the datasets, whereas several of the time series on the south coast showed co-occurrence for their most extreme MHWs. Interestingly, the rates of co-occurrence for these largest MHWs was greater when the *in situ* event preceded the OISST event.

3.4. Decadal trends in MHWs and MCSs

In order to calculate the decadal trends in MHW and MCS count, linear models were fitted to the annual count values for each 30+ year time series. The slope of this line was then multiplied by ten to produce the following decadal trend values and show whether after 30+ years MHWs/ MCSs are increasing or decreasing. As the OISST data set is over 30 years in duration, decadal values were calculated for each OISST time series. It was found that the mean(sd) decadal trend for MHW occurrence in the OISST dataset was 0.5(0.3) dec^{-1} across all sites and -0.7(0.6) dec^{-1} for MCSs. The decadal trends in MHW occurrence increase as one moves from the colder Benguela fed west coast to warmer Agulhas fuelled east coast with the mean(sd) decadal MHW trend on the west coast being 0.3(0.3) dec^{-1}, the south coast being 0.5(0.3) dec^{-1} and the east coast coming in at 0.6(0.2) dec^{-1}. Just as MHWs are occurring more frequently per decade on the east coast than the west, MCSs are decreasing more frequently on the east coast than the west. The decadal trend in MCSs on the west coast is -0.1(0.6) dec^{-1}, -0.8(0.5) dec^{-1} on the south coast and -0.9(0.2) dec^{-1} on the east coast.

Of the 21 *in situ* time series, only 4 of them reached the 30+ year requirement. Of these four time series the mean(sd) decadal trend for MHWs was found to be 0.3(0.5) dec^{-1} and -0.1(0.5) dec^{-1} for MCSs. There were two sites from the west coast and two from the south, excluding the east coast from a possible calculation of decadal change for *in situ* MHWs and MCSs. The mean(sd) decadal

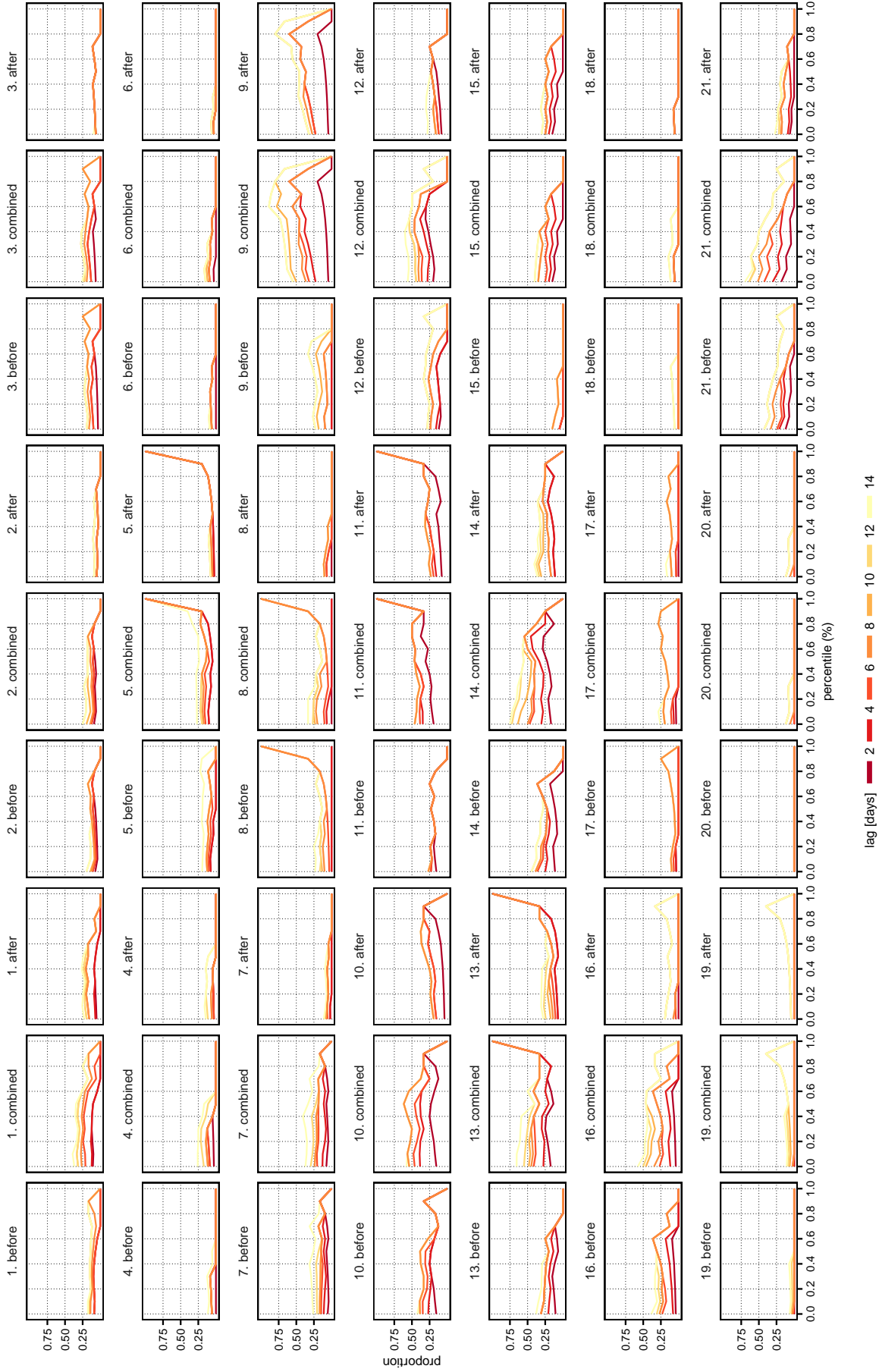Perhaps the trends here would be better shown as a table?

15

Figure 4: Proportion of MHW co-occurrence between *in situ* and OISST datasets for each site where sites 1 − 4 represent the west coast, sites 5 − 17 the south coast and 18 − 21 the east coast. The left column denotes the proportion of co-occurrence when events in the OISST data occurring on or before the dates of the *in situ* events were used. The left column shows the proportion of co-occurrence when OISST events that occurred after the *in situ* event dates were compared. The central column shows the overall proportion of co-occurrence. The *x*-axis indicates the size of the events, based on percentiles, used for calculating the co-occurrence proportions. The days of lag used, from 2 − 14, are shown here in diminishing shades of red.
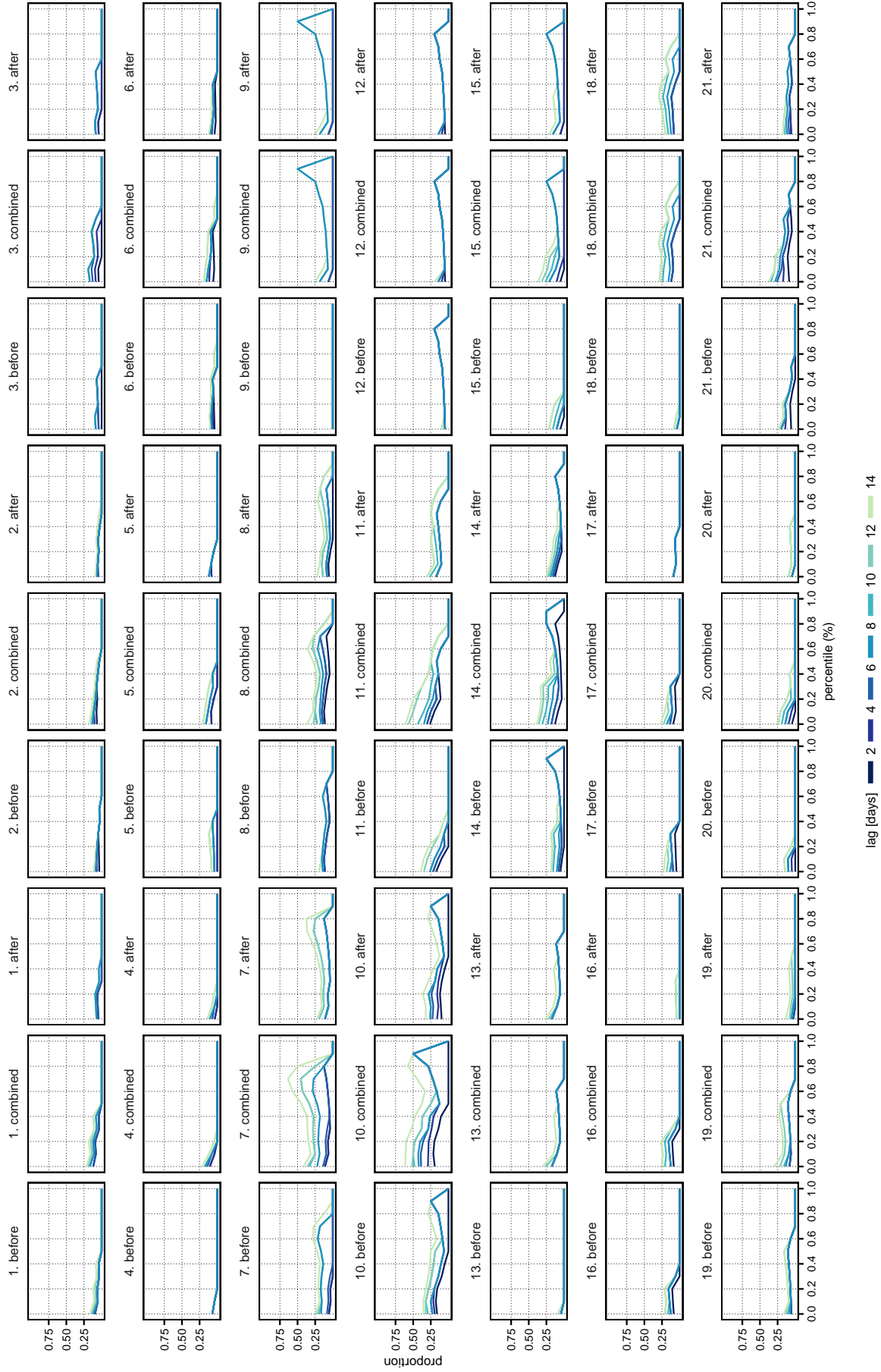
Figure 5: Proportion of MCS co-occurrence between *in situ* and OISST datasets for each site as seen for MHWs in Figure 4. The days of lag are shown here in diminishing shades of blue.

trend for MHWs (MCSs) on the west coast was 0.1(0.5) dec^{-1} (-0.2(0.7) dec^{-1}) and 0.5(0.5) dec^{-1} (0.1(0.4) dec^{-1}) on the south.

For the remaining 17 *in situ* time series we calculated the the sum of the annual count of events
in the first half of each time series compared against the sum of the annual count of events in the second half. This produced a proportion value that could be used as an indicator as to how many more MHWs or MCSs were occurring in the second half of the time series. The mean(sd) proportion of MHWs occurring in the second half of the shorter time series was 1.7(1.3) whereas the proportion of MCSs was 0.8(0.6), meaning that more of the MHWs are occurring in the second half of time series than the first, and vice versa for the MCSs. The shorter time series on the south coast showed the pattern of having more MHWs in the second half of the time series at 2.1(1.4) and fewer MCSs in the second half at 0.5(0.3). The short west coast time series had more MHWs in the second half at 1.5(0.6) as well as more MCSs at 1.8(0.6). The east coast had fewer MHWs at 0.7(0.4) in the second half of the shorter time series with the proportion of MCSs in being roughly split between the first and second half of the time series at 1.0(0.8).

4. Discussion

4.1. Events

Though it could be expected due to the design of the Hobday et al. (2016) MHW framework, it was not yet known that every time series from each coastal section of South Africa has experienced on average more than one MHW and one MCS per year. It was surprising to find that the mean intensity of MCSs on the south coast was significantly larger ($p<0.01$) than the west coast, which is in an EBUS. From these results we may now hypothesise that there is an additional driver on the south coast affecting the extreme events there that is not present on the other two coastal sections. It was assumed that the east coast would experience the fewest and least intense events. Whereas the duration (days) of its events were significantly shorter than the south coast ($p<0.01$), the count and mean intensity of its MHWs and MCSs were not the smallest found. This means that every section of the coast has the potential to experience an event strong enough to affect its species assemblage and/or local ecology.

The difference between the *in situ* and OISST datasets was also striking. One may see in Table 2 and Table 3 that the patterns presented by the data are intrinsically different, it is not simply a matter of the statistical significance between the values. The OISST data showed many weak events occurring often whereas the *in situ* dataset showed fewer, stronger events. This implies that a large number of the events occurring between these two datasets are unrelated and that some other variable may be having a more pronounced effect on the coast than ocean temperature. Besides this difference, both datasets tended to show that the south coast had longer and more intense events than the other two coastal sections, but this too is not a consistent result. Before calculating the proportions of co-occurrence, it was already clear from these results that the events that occurred within the OISST data would differ from the *in situ* data.
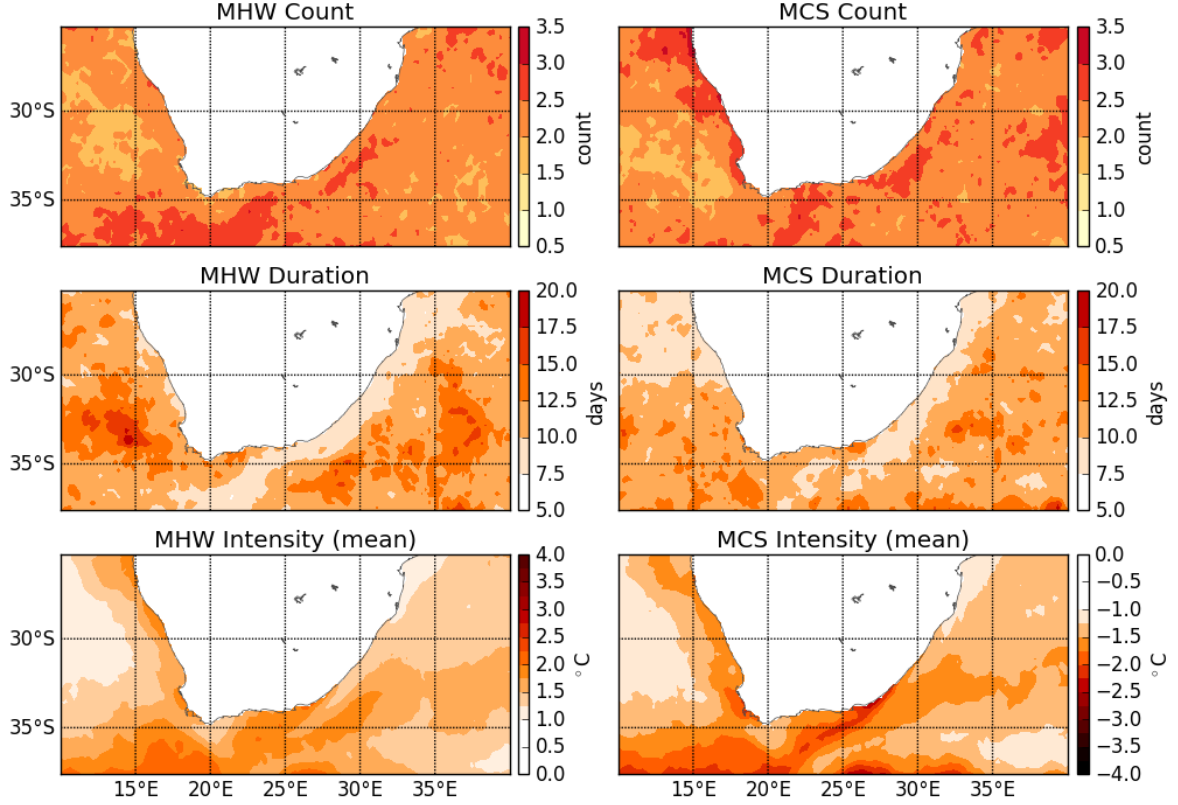
Figure 6: Mean values from the annual data of each pixel from the OISST dataset around southern Africa. The first second and third rows show the mean count, duration (days) and intensity (°C) respectively of MHWs in the first column and MCSs in the second. The annual event values within each pixel were meaned to create one final value with which each pixel is populated. The "MCS Intensity (mean)" panel shows the intensity of the MCSs in negative values, not absolute values.

When ones gaze is turned away from the coast at the ocean around southern Africa more broadly, the meso-scale patterns as they occur independent of the continent may be more readily seen. Figure 6 shows the mean count, duration (days), and intensity (°C) of each pixel from the OISST dataset as derived from the annual data. These data show that the most MHWs occur well south of the tip of the continent whereas some of the most frequent MCS activity may be found directly against the west coast. This helps to explain the finding that MHWs were shown to be longer and more intense in the *in situ* dataset, whereas the OISST dataset shows MCSs being longer and more intense. As for the duration of events, it is clear from Figure 6 that the MHWs and MCSs the satellite is detecting in the Agulhas current are relatively short. Almost all of the pixels that show events in the upper range of the durations detected occurred well away from the coast, too. This explains why the events in the *in situ* data have greater durations. As for the intensity of offshore events, the west and south coasts are shown to have centres of intensity very near the shore whereas the east coast generally does not. The most intense events detected in the OISST data where found to occur along or below the south coast. This helps to explain why the south coast showed the greatest proportion of co-occurrence for the three coastal sections, with the west coast second.

One may see in the z-axis in Figure 6 that the range of count, days and intensities is similar to that found in the *in situ* data, but that these larger events are generally occurring farther from the coast. This supports the argument that the events detected along the coast by these two different datasets were not the same, even when they were found to occur within similar time frames. It was also counter-intuitive to find that the OISST data showed stronger MCSs than the *in situ* data. One would assume that as the *in situ* data are measured at *ca.* 5m deep on average, which is below the bulk surface layer (*ca.* 0.5m) that the OISST data measure (Reynolds et al., 2002), they would be predisposed to picking up cold upwelling events and less exposed to thermal heating, which would appear as larger MCSs and smaller MHWs compared to the OISST data. The cause of this discrepancy warrants further research.

This apparent discrepancy also places doubt on the use of MCSs as a proxy for upwelling. If the *in situ* data had recorded longer and/or more intense MCSs than the OISST data it would have shown that the MCS algorithm was detecting more extreme cold events near the coast, where upwelling is known to occur (Lutjeharms et al., 2000; Hutchings et al., 2009). Instead the results show that offshore MCS are, on average, longer and more intense. It is the suggestion of the authors that using the MCS algorithm to detect upwelling be done with extreme caution. The MCS algorithm detects cold events based on their intensity outside of a locally produced climatology, and because most upwelling occurs at seasonally predictable times, the cold events detected here are likely due to other factors. Aside from this observation, upwelling events should have notable properties, such as rate of onset and duration of peak intensity, which set them apart from other events that may cause colder water to occur at the surface. Further work on the definition of the characteristics of upwelling events could be coupled with the MCS algorithm for accurate use in upwelling detection in temperature time series.

4.2. Top three events

It was hypothesised that the south coast would experience the most extreme events as measured by cumulative intensity, but it was unanticipated that these events would be so much larger than the other two coastal sections. Conversely, it was hypothesised that the east coast would experience the least extreme events and this proved to be correct.

The disagreement between the *in situ* and OISST datasets continued into the detection of the top three events for each coastal section. The pattern of event sizes within the *in situ* data are very clear in that events on the south coast are much more extreme than the west and east coasts in that order. The OISST data are less conclusive on whether the south or west coast experiences the most extreme events, but it is apparent from all of the analyses from both datasets that the east coast experiences very few extreme MHWs or MCSs. Indeed, these findings support the hypothesis that the east coast is the most stable of the three coasts as both datasets show the most extreme events occurring here to only be a factor of two greater than the coastal mean for cumulative intensity.

The sites along the south coast could be further divided into those within False Bay (Sites 5–7) and those on the Agulhas Bank (Sites 8–17). False Bay, which is ~50 km across, is situated within the transition zone between the Benguela and Agulhas Currents (Smit et al., 2013). Many satellite

temperatures products therefore inadequately resolve the SST within this body of water (cite.). This is problematic as it is important to precisely monitor the large ranges in temperature this area experiences (cite.) as it is important both ecologically (cite.) and to the many stakeholders that use this embayment. Two of the three largest MHWs and MCSs from the *in situ* dataset were recorded within False Bay,

₄₄₅ whereas only one large MHW and no MCSs were detected with the OISST dataset. This illustrates the problem of using satellite temperature data for coastal ecology.

The example of the discrepancies for the size of the events recorded in False Bay also serves to illustrate the usefulness of satellite SST data to detect events near the coast. For example, Roberts (2005) argues for a wind forced coastal upwelling cell near Tsitsikamma (Sites 12–14). That these three

₄₅₀ sites show greater cumulative intensities for MCSs than all but one time series from the OISST dataset may support the hypothesis of such a coastal upwelling cell. Though as mentioned earlier, the current MCS algorithm should not be taken as showing upwelling events with any fidelity. More research is necessary if upwelling hypotheses like the aforementioned may be investigated in this manner. This would be an intriguing use of the MCS algorithm to validate multiple competing hypotheses that as of

₄₅₅ yet may not have been able to be tested in any other way.

Another important consideration was the co-occurrence of the most extreme events between and within time series. As one may see in Table 4 and Table 5, none of the top three MHWs or MCSs for any of the coastal sections from the *in situ* dataset were the same. They were all individually different events occurring at different times. The OISST dataset tells an entirely different story in

₄₆₀ that all but one of the coastal sections for both MHWs and MCSs, had at least two of the three top events occurring at the same time. This means that the largest events detected in the OISST data were occurring over a broad area at the same time whereas the *in situ* events were isolated not only in time, but in the location in which they were occurring. This further reinforces our conclusion that the events detected by the different datasets are often intrinsically different from one another.

₄₆₅ *4.3. Co-occurrence rates*

As one may see in Figure 4, when looking at the lag window before the *in situ* events occurred, the rates of co-occurrence for MCSs are much lower than for the MHWs. This shows that if these events are indeed related, more MHWs are being caused by meso-scale activity than MCSs, as was expected. This finding is supported further by comparing the rates of co-occurrence for MCS lagged before and

₄₇₀ after the *in situ* event occurred. More MCS from the OISST data are shown to occur after the *in situ* events for all coastal sections. The co-occurrence rates of MHWs before and after the *in situ* events are similar.

One may also infer from the results that the proportions of co-occurrence for time series on the south coast being much larger than the other two coasts is caused by the much higher level of influence from

₄₇₅ meso-scale phenomena occurring on the Agulhas Bank. We also see that there is a higher proportion of co-occurrence for the larger MHWs and MCSs on the south coast when a lag window after the *in situ* event is used (Figure 4). This supports the argument that events originating in the nearshore are then propagating out onto the Agulhas Bank and affecting the oceanography there more often

than meso-scale events originating on the Agulhas Bank are affecting the nearshore environment. The overall low rates of co-occurrence for all three coastal sections reinforces the argument that it is not the meso-scale phenomena of the open ocean abutting the southern African landmass that are driving extreme events in the nearshore.

The very low proportion of co-occurrence between the datasets, and the decline in the proportion as the smaller events are screened out is strong evidence against the hypothesis that meso-scale activity, both warm and cold, is causing nearshore extreme thermal events. The small increases in co-occurrence for some sites as only larger events were compared does imply that there is some relationship between the inshore and offshore, but that some other variable (e.g. atmospheric forcing) may be having a greater effect on inshore events.

4.4. Climate change

As MHWs and MCSs are temperature related phenomena we would be remiss not to discuss the potential of our findings in relation to climate change. The count of the MHWs and MCSs that occurred along the coast is less telling in this regard than the trend in these events themselves. Although all but 4 of the *in situ* time series used in this investigation are too short to draw adequate conclusions on the decadal trends seen in MHWs and MCSs, the OISST data are not. And as hypothesised these data showed positive decadal trends for MHWs and negative trends for MCSs. Meaning that over the past 33 years of satellite observation along the shore-normal transects seen in Figure 1, MHWs have been increasing every decade for each coastal section while MCSs have been decreasing. When one looks more broadly at the ocean around southern Africa this pattern generally holds up. One may see in Figure 7 that the count, duration and intensity of MHWs have almost exclusively been increasing throughout the studied regions of the Indian and Atlantic oceans. The count of MCS has been decreasing most rapidly along the coast of southern Africa with a couple of notable exceptions near Port Elizabeth and north of the Cape Peninsula where the count of MCSs have been increasing very near to the coast. The duration of MCSs is seen to generally increase further offshore with most of the nearshore changing little or decreasing. The intensity of MCSs is either changing little near the coast or is increasing dramatically, as seen in the dark blue spot north of the Cape Peninsula in the "MCS Intensity (mean) Trend" panel in Figure 7. This means that a consistent 30+ year trend in extreme cold events, more so than anywhere else in this region of the ocean, has been acting on the coastal waters here. Investigations into the impact this may have had on the ecosystems here may produce interesting findings in regards to the effect of climate change on ecosystems.

Though less conclusive than the trends calculated from the longer time series, similar patterns were found in the shorter *in situ* time series as well. As the algorithm used to calculate these events is based on percentiles, it stands to reason that as the mean temperature of South Africa's coastal waters has been increasing by 0.1°C per decade on average since the early 1970's (Schlegel and Smit, in review), there will be an increase in MHWs and a decrease in MCSs. The gradual mean increase in temperature will cause the algorithm used here to be biased in its detection of MHWs as time progresses simply because temperatures are generally warmer in the later half of the time series therefore, the chances of
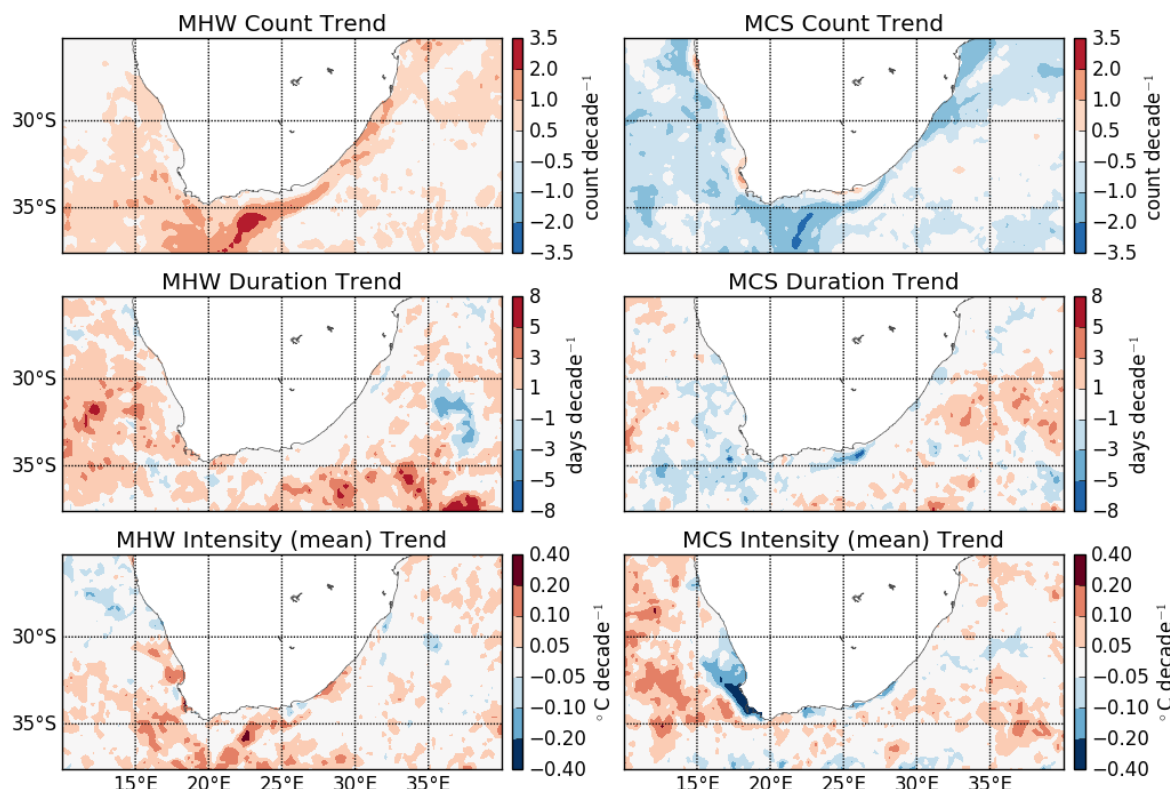
22

Figure 7: Decadal trend values calculated from the annual OISST data around southern Africa. The decadal trends were calculated by fitting a linear model to the annual data of each pixel for the relevant metrics and multiplying the slope of the line by 10. The panels are in the same position as Figure 6. The "MCS Intensity (mean) Trend" panel shows the trend in MCS intensity as negative values, not absolute values (e.g. dark blue regions mean the MCSs are getting stronger, not weaker).

the algorithm detecting a MHW increases because the base temperature from which the MHW will be fluctuating from will be greater than the beginning of the time series. Ultimately, for the species and ecosystems experiencing this increase in duress, the semantic argument of the viability of percentiles provides little solace.

> Nice concluding statement here!

5. Conclusion

Given that the MHW algorithm is based on the percentiles found within each time series and not on arbitrarily decided minimum or maximum thresholds, one will always find a certain number of MHWs and MCSs in any time series. This is evident in the results of our analysis (Table 2 and Table 3) in that every time series used from both datasets experiences on average at least one MHW and MCS per year. Within each dataset, but not between, the count of events are similar for each coastal section, regardless of the local oceanographic and geographic properties. It is the cumulative intensity of the events occurring on the different coastal sections that most clearly defines them. We expected to see the most intense MCSs on the west coast as this is part of an EBUS however, the south coast, a region dominated by the warmer Agulhas Current, but with some influence from the colder Benguela, had

23

both the most intense and longest MHWs and MCS in the *in situ* data. Even though it had been hypothesized that the south coast would have intense events, the magnitude of intensity of the events that occurred here over the other coastal sections was surprising.

We have also shown that MCSs are not a good indicator for upwelling. As upwelling tends to occur at seasonally predictable times, the MCS algorithm does not consider these events as anomalous. Therefore the MCSs measured here are indicators of non-seasonal or atypical forcing.

As the rates of co-occurrence between *in situ* and OISST data are generally low, and the magnitude and co-occurrence of events within the different datasets differ from one another, we infer that some other force outside of meso-scale phenomena is contributing to extreme inshore events. This is likely due to atmospheric forcing and warrants further research to better understand what is driving the occurrence and intensity of these events.

Supplementary

Meta-data

Further meta-data for each time series and source listed in geographic order along the South African coast from the border of Namibia to the border of Mozambique may be found in Table S1.

References

Alexander, L. V., Zhang, X., Peterson, T. C., Caesar, J., Gleason, B., Klein Tank, A. M. G., Haylock, M., Collins, D., Trewin, B., Rahimzadeh, F., Tagipour, A., Rupa Kumar, K., Revadekar, J., Griffiths, G., Vincent, L., Stephenson, D. B., Burn, J., Aguilar, E., Brunet, M., Taylor, M., New, M., Zhai, P., Rusticucci, M., Vazquez-Aguirre, J. L., 2006. Global observed changes in daily climate extremes of temperature and precipitation. Journal of Geophysical Research Atmospheres 111 (5).

American Meteorological Society, 2011. American Meteorological Society Glossary of Meteorology.

Black, E., Blackburn, M., Harrison, R. G., Hoskins, B. J., Methven, J., 2004. Factors contributing to the summer 2003 European heatwave. Weather 59 (8), 217–223.

Table S1: The metadata and coastal averages for all *in situ* time series used in this study.

ID	site	coast	lon	lat	start date	end date	duration (years)	NA %	mean	sd	min	max
1	Port Nolloth	west	16.87	-29.25	1973-07-22	2011-08-31	38.1	6.8	12.3	1.4	9.2	21.0
2	Sea Point	west	18.38	-33.92	1973-12-31	2011-08-10	37.6	6.3	13.1	1.6	8.7	23.0
3	Hout Bay	west	18.35	-34.05	1991-03-25	2008-04-21	17.1	4.9	11.2	1.8	7.5	16.7
4	Kommetjie	west	18.33	-34.14	1992-02-29	2011-08-17	19.5	7.4	13.3	1.6	9.0	20.4
coast	mean	west					28.1	6.3	12.5	1.6	8.6	20.3
5	Fish Hoek	south	18.44	-34.14	1992-02-29	2011-08-17	19.5	5.9	15.4	2.3	10.0	22.5
6	Muizenberg	south	18.48	-34.10	1973-05-04	2011-08-24	38.3	3.9	15.9	3.0	9.0	25.0
7	Gordons Bay	south	18.86	-34.16	1972-09-12	2011-08-24	39.0	4.0	16.5	2.4	10.0	25.5
8	Hermanus	south	19.25	-34.41	1989-11-30	2011-05-18	21.5	4.1	15.6	1.6	9.0	23.5
9	Ystervarkpunt	south	21.74	-34.40	1995-10-23	2007-06-19	11.7	0.0	17.6	2.6	10.1	23.6
10	Mossel Bay	south	22.16	-34.18	1991-06-26	2007-06-19	16.0	8.4	18.0	2.7	10.1	24.6
11	Knysna	south	23.07	-34.08	1995-03-21	2009-11-04	14.6	6.3	17.3	2.6	10.7	24.2
12	Tsitsikamma West	south	23.65	-33.98	1990-06-30	2007-02-14	16.6	7.7	17.2	2.6	9.5	29.3
13	Storms River Mouth	south	23.90	-34.02	1993-03-31	2008-12-30	15.8	4.0	16.8	2.5	9.4	24.4
14	Tsitsikamma East	south	23.91	-34.03	1991-06-29	2009-11-08	18.4	4.0	16.8	2.5	8.8	23.4
15	Pollock Beach	south	25.68	-33.99	1999-05-12	2011-07-06	12.2	3.0	18.1	2.1	10.8	26.5
16	Humewood	south	25.65	-33.97	1973-08-24	1999-12-30	26.4	3.1	18.0	2.3	11.0	25.0
17	Hamburg	south	27.49	-33.29	1995-10-30	2010-02-25	14.3	6.4	17.5	1.8	12.1	24.1
coast	mean	south					20.3	4.7	17.0	2.4	10.0	24.7
18	Eastern Beach	east	27.92	-33.02	1983-12-31	1998-07-30	14.6	9.8	17.9	1.8	12.5	25.0
19	Orient Beach	east	27.92	-33.02	1983-12-31	2011-07-06	27.5	3.9	18.0	1.6	12.0	26.0
20	Nahoon Beach	east	27.95	-32.99	1983-12-31	1998-07-30	14.6	7.0	18.1	1.7	10.0	25.0
21	Sodwana	east	32.73	-27.42	1994-03-11	2010-01-25	15.9	7.0	24.4	2.0	18.6	29.1
coast	mean	east					18.2	6.9	19.6	1.8	13.3	26.3

Bond, N. A., Cronin, M. F., Freeland, H., Mantua, N., 2015. Causes and impacts of the 2014 warm anomaly in the NE Pacific.

Castillo, K. D., Lima, F. P., 2010. Comparison of in situ and satellite-derived (MODIS-Aqua/Terra) methods for assessing temperatures on coral reefs. Limnology and Oceanography Methods 8, 107–117.

Chen, K., Gawarkiewicz, G., Kwon, Y.-O., Zhang, W. G., 2015. The role of atmospheric forcing versus ocean advection during the extreme warming of the Northeast U.S. continental shelf in 2012. Journal of Geophysical Research: Oceans 120, 1–16.

Chen, K., Gawarkiewicz, G. G., Lentz, S. J., Bane, J. M., 2014. Diagnosing the warming of the Northeastern U.S. Coastal Ocean in 2012: A linkage between the atmospheric jet stream variability and ocean response. Journal of Geophysical Research: Oceans 119 (1), 218–227.

Crisp, D. J., 1964. The effects of the severe winter of 1962-63 on marine life in Britain. Journal of Animal Ecology 33 (1), 165–210.

DeCastro, M., Gõmez-Gesteira, M., Costoya, X., Santos, F., 2014. Upwelling influence on the number of extreme hot SST days along the Canary upwelling ecosystem. Journal of Geophysical Research: Oceans 119 (5), 3029–3040.

Easterling, D. R., Meehl, G. A., Parmesan, C., Changnon, S. A., Karl, T. R., Mearns, L. O., 2000. Climate Extremes: observations, modeling, and impacts. Science 289 (5487), 2068–2074.

Ellis, J. M., 2015. A Quantitative Assessment of the January 2010 Cold Spell Effect on Mangrove Utilizing Coral Reef Fishes from Biscayne National Park, Florida.

Feng, M., McPhaden, M. J., Xie, S.-P., Hafner, J., 2013. La Niña forces unprecedented Leeuwin Current warming in 2011. Scientific reports 3, 1277.

Firth, L. B., Knights, A. M., Bell, S. S., 2011. Air temperature and winter mortality: Implications for the persistence of the invasive mussel, Perna viridis in the intertidal zone of the south-eastern United States. Journal of Experimental Marine Biology and Ecology 400 (1-2), 250–256.

Firth, L. B., Mieszkowska, N., Grant, L. M., Bush, L. E., Davies, A. J., Frost, M. T., Moschella, P. S., Burrows, M. T., Cunningham, P. N., Dye, S. R., Hawkins, S. J., 2015. Historical comparisons reveal multiple drivers of decadal change of an ecosystem engineer at the range edge. Ecology and Evolution 5 (15), 3210–3222.

Fischer, E. M., Lawrence, D. M., Sanderson, B. M., 2011. Quantifying uncertainties in projections of extremes - a perturbed land surface parameter experiment. Climate Dynamics 37 (7-8), 1381–1398.

Fischer, E. M., Schär, C., 2010. Consistent geographical patterns of changes in high-impact European heatwaves. Nature Geoscience 3 (6), 398–403.

García-Reyes, M., Sydeman, W. J., Schoeman, D. S., Rykaczewski, R. R., Black, B. a., Smit, A. J., Bograd, S. J., 2015. Under Pressure: Climate Change, Upwelling, and Eastern Boundary Upwelling Ecosystems. Frontiers in Marine Science 2 (December), 1–10.

Garrabou, J., Coma, R., Bensoussan, N., Bally, M., Chevaldonné, P., Cigliano, M., Diaz, D., Harmelin, J. G., Gambi, M. C., Kersting, D. K., Ledoux, J. B., Lejeusne, C., Linares, C., Marschal, C., Pérez, T., Ribes, M., Romano, J. C., Serrano, E., Teixido, N., Torrents, O., Zabala, M., Zuberer, F., Cerrano, C., 2009. Mass mortality in Northwestern Mediterranean rocky benthic communities: Effects of the 2003 heat wave. Global Change Biology 15 (5), 1090–1103.

Gershunov, A., Douville, H., 2008. Extensive summer hot and cold extremes under current and possible future climatic conditions: Europe and North America. In: Climate Extremes and Society. pp. 74–98.

Gunter, G., 1941. Death of Fishes Due to Cold on the Texas Coast, January, 1940. Ecology 22 (2), 203–208.

Gunter, G., 1951. Destruction of Fishes and Other Organisms on the South Texas Coast by the Cold Wave of January 28-February 3, 1951. Ecology 32 (4), 731–736.

Hobday, A. J., Alexander, L. V., Perkins, S. E., Smale, D. A., Straub, S. C., Oliver, E. C., Benthuysen, J. A., Burrows, M. T., Donat, M. G., Feng, M., Holbrook, N. J., Moore, P. J., Scannell, H. A., Sen Gupta, A., Wernberg, T., feb 2016. A hierarchical approach to defining marine heatwaves. Progress in Oceanography 141, 227–238.

Holt, S. A., Holt, G. J., 1983. Cold Death of Fishes at Port Aransas, Texas: January 1982. The Southwestern Naturalist 28 (4), 464–466 CR – Copyright © 1983 Southwestern A.

615 Hutchings, L., van der Lingen, C. D., Shannon, L. J., Crawford, R. J. M., Verheye, H. M. S., Bartholomae, C. H., van der Plas, a. K., Louw, D., Kreiner, A., Ostrowski, M., Fidel, Q., Barlow, R. G., Lamont, T., Coetzee, J., Shillington, F., Veitch, J., Currie, J. C., Monteiro, P. M. S., 2009. The Benguela Current: An ecosystem of four components. Progress in Oceanography 83 (1-4), 15–32.

Jentsch, A., Kreyling, J., Beierkuhnlein, C., 2007. A New Generation of Climate-Change Experiments: 620 Events, Not Trends 9295 (November 2015).

Kreyling, J., Beierkuhnlein, C., Ellis, L., Jentsch, A., 2008. Invasibility of grassland and heath communities exposed to extreme weather events - Additive effects of diversity resistance and fluctuating physical environment. Oikos 117 (10), 1542–1554.

Lima, F. P., Wethey, D. S., 2012. Three decades of high-resolution coastal sea surface temperatures 625 reveal more than warming. Nature Communications 3, 704.

Lüning, K., 1990. Seaweds: their environment, biogeography and ecophysiology. Jhon Wiley and Sons. Wiley, New York (USA).

Lutjeharms, J. R. E., Cooper, J., Roberts, M., 2000. Upwelling at the inshore edge of the Agulhas Current. Continental Shelf Research 20 (7), 737–761.

630 Mackenzie, B. R., Schiedek, D., 2007. Daily ocean monitoring since the 1860s shows record warming of northern European seas. Global Change Biology 13 (7), 1335–1347.

Marsh, H., O'Shea, T. J., Best, R. C., 1986. Research on Sirenians. Ambio 15 (3), 177–180.

Matthes, H., Rinke, A., Dethloff, K., 2015. Recent changes in Arctic temperature extremes: warm and cold spells during winter and summer. Environmental Research Letters 10 (11), 114020.

635 Meehl, G. a., 2004. More Intense, More Frequent, and Longer Lasting Heat Waves in the 21st Century. Science 305 (5686), 994–997.

Mills, K. E., Pershing, A. J., Brown, C. J., Chen, Y., Chiang, F.-S., Holland, D. S., Lehuta, S., Nye, J. a., Sun, J. C., Thomas, A. C., Wahle, R. a., 2012. Lessons From the 2012 Ocean Heat Wave in the Northwest Atlantic. Oceanography 26 (2), 60–64.

640 Olita, A., Sorgente, R., Natale, S., Gaberšek, S., Ribotti, A., Bonanno, A., Patti, B., 2007. Effects of the 2003 European heatwave on the Central Mediterranean Sea: surface fluxes and the dynamical response. Ocean Science 3 (2), 273–289.

O'Shea, T. J., Beck, C. A., Bonde, R. K., Kochman, H. I., Odell, D. K., 1985. An analysis of manatee mortality patterns in Florida, 1976-81. The Journal of Wildlife Management 49 (1), 1–11.

645 Pachauri, R. K., Meyer, L., Van Ypersele, J.-P., Brinkman, S., Van Kesteren, L., Leprince-Ringuet, N., Van Boxmeer, F., 2014. Climate Change 2014 Synthesis Report.

27

Pearce, A. F., Feng, M., 2013. The rise and fall of the "marine heat wave" off Western Australia during the summer of 2010/2011. Journal of Marine Systems 111-112, 139–156.

Perkins, S. E., Alexander, L. V., 2013. On the measurement of heat waves. Journal of Climate 26 (13), 4500–4517.

Rehage, J. S., Blanchard, J. R., Boucek, R. E., Lorenz, J. J., Robinson, M., 2016. Knocking back invasions: variable resistance and resilience to multiple cold spells in native vs. nonnative fishes. Ecosphere 00 (00), e01268.

Reynolds, R. W., Rayner, N. A., Smith, T., 2002. An improved in situ and satellite SST analysis for climate. Journal of Climate.

Reynolds, R. W., Smith, T. M., Liu, C., Chelton, D. B., Casey, K. S., Schlax, M. G., 2007. Daily high-resolution-blended analyses for sea surface temperature. Journal of Climate 20 (22), 5473–5496.

Roberts, M. J., 2005. Chokka squid (Loligo vulgaris reynaudii) abundance linked to changes in South Africa's Agulhas Bank ecosystem during spawning and the early life cycle. ICES Journal of Marine Science 62 (1), 33–55.

Selig, E., Casey, K., Bruno, J. F., 2010. New insights into global patterns of ocean temperature anomalies: implications for coral reef health and management. Global Ecology and Biogeography 9999 (9999).

Smale, D. A., Wernberg, T., 2009. Satellite-derived SST data as a proxy for water temperature in nearshore benthic ecology Peer reviewed article. Marine Biology 387, 27–37.

Smit, A. J., Roberts, M., Anderson, R. J., Dufois, F., Dudley, S. F. J., Bornman, T. G., Olbers, J., Bolton, J. J., 2013. A coastal seawater temperature dataset for biogeographical studies: Large biases between in situ and remotely-sensed data sets around the coast of South Africa. PLoS ONE 8 (12).

Sura, P., 2011. A general perspective of extreme events in weather and climate. Atmospheric Research 101 (1-2), 1–21.

Wernberg, T., Russell, B. D., Moore, P. J., Ling, S. D., Smale, D. A., Campbell, A., Coleman, M. A., Steinberg, P. D., Kendrick, G. A., Connell, S. D., 2011. Impacts of climate change in a global hotspot for temperate marine biodiversity and ocean warming. Journal of Experimental Marine Biology and Ecology 400 (1-2), 7–16.

Wernberg, T., Smale, D. A., Tuya, F., Thomsen, M. S., Langlois, T. J., de Bettignies, T., Bennett, S., Rousseaux, C. S., 2013. An extreme climatic event alters marine ecosystem structure in a global biodiversity hotspot. Nature Climate Change 3 (1), 78–82.

Woodward, F. I., 1987. Climate and Plant Distribution.